Equilibrium and kinetics of local ordering in Ni(Al) solid solutions

1990 J. Phys.: Condens. Matter 2 7061

(http://iopscience.iop.org/0953-8984/2/34/001)

J. Phys.: Condens. Matter **2** (1990) 7061–7075. Printed in the UK

Equilibrium and kinetics of local ordering in Ni(Al) solid solutions

B Sitaud and O Dimitrov
CECM–CNRS, 15 rue G Urbain, 94407 Vitry-sur-Seine Cédex, France

Received 26 May 1989, in final form 1 May 1990

Abstract. Short-range order has been investigated in Ni(Al) solid solutions (with 6 and 10 at.% Al) by measurements of the residual electrical resistivity during thermal treatments. Local ordering results in an increase of resistivity, much stronger for the higher Al concentration. During isothermal annealing, the asymptotic residual resistivity, which characterises the equilibrium state of short-range order, was found to be a linear function of reciprocal temperature. In conditions of constant vacancy concentration, the approach to equilibrium could not be consistently represented by first-order kinetics, even with a distribution of relaxation times or by a sum of two exponentials. Indeed, for the 10 at.% Al alloy, the results clearly proved that the time constant was amplitude-dependent. Although a so-called cross-over was observed in that alloy, the quantitative evaluation of the relaxation of short-range order was carried out by application of a power law. The activation enthalpies of self-diffusion obtained lie in the same range as published diffusion data and they appear to increase when Al concentration goes from 6 to 10 at.%.

1. Introduction

Among the studies devoted to nickel-base superalloys, composed of a γ' hardening phase in a γ matrix, only a few have been concerned with the properties of point defects. However, these parameters are clearly important since they directly control the atomic mobility and so the structural stability and the excellent mechanical properties at high temperature (creep).

Ni(Al) solid solutions represent a model for the γ matrix of such alloys. In these materials, like in several binary concentrated alloys, the atoms do not randomly occupy the lattice sites. The existence of short-range ordering was clearly proved by various experimental methods (Guy 1962, Starke *et al* 1965, Katsnel'son *et al* 1972, 1977), and more recently the Warren–Cowley parameters α_i (Cowley 1950) for three compositions and at four temperatures were obtained from x-ray scattering experiments (Chassagne 1986, Klaiber *et al* 1987). According to these different sources of information short-range order (SRO) increases between 3 at.% Al and 10 at.% Al.

Since the changes of SRO (which only require a few elementary atom jumps) are diffusion-controlled, the rate of ordering should be proportional to the product of the concentration and the jump frequency of point defects. Therefore, the investigation of the kinetics of SRO formation in such concentrated alloys should yield information first on the ordering process itself and secondly on the behaviour of point defects.

0953-8984/90/347061 + 15 $03.50

To investigate SRO kinetics a direct approach consists of determining the SRO structure by scattering experiments at a given temperature as a function of time. This supposes a large number of measurements, which are not easily performed by such methods. Another solution is to follow a physical property affected by the SRO evolution. The most used is electrical resistivity, which allows one to obtain the results with more simplicity and accuracy. Nevertheless such measurements could only be considered as macroscopic information compared with the determination of each Warren–Cowley parameter. Indeed the different effects contributing to the variations of the electrical resistivity are difficult to separate. This has led to the development of several kinetic models for predicting the evolution of SRO.

In the present paper, the SRO variations in two Ni(Al) alloys (6 at.% Al and 10 at.% Al) have been investigated by measurements of residual electrical resistivity. In a suitable range of annealing temperatures, the kinetics were recorded after sudden small temperature changes, in order to be rapidly in conditions of constant equilibrium vacancy concentration. The applicability of formal models of ordering kinetics was considered, particularly in view of the amplitude dependence found for the relaxation rates, to obtain information on the self-diffusion. Until now the influence of relaxation amplitude had not been taken into account in this system (Afyouni *et al* 1989).

2. Experimental details

The materials used in the present experiments were nickel alloys containing 6.0 and 10.0 at.% Al. Weighed quantities of nickel (99.9985%) and aluminium (99.9999%) were melted in an inductive plasma furnace. The uncertainty on the Al concentration was smaller than 0.1%. Resulting ingots of about 5 g were homogenised at 1273 K for 24 h in a 10^{-8} Torr vacuum. X-ray diffraction analyses on sheet samples after a normalisation anneal (30 min at 1273 K, furnace cooling) showed a single FCC phase with lattice parameters in agreement with those reported by Chassagne (1986).

To check the stability of the γ phase in the Ni-10 at.% Al alloy, which is near to the γ–γ' solubility limit of the phase diagram (Hansen and Anderko 1958, Sanchez *et al* 1984), specific characterisations were performed by transmission electron microscopic observations, to try and detect the existence of Ni_3Al precipitates, and by Curie temperature measurements, which are sensitive to a change in the Al content of the γ phase. The comparison between a sample quenched from 1273 K (i.e. well within the single-phase field) and an aged sample (quenched from 1273 K and annealed at 660 K for 435 h) did not show any indication of the formation of γ' precipitates.

Specimens for electrical resistivity measurements were cold drawn to wires of two different geometries: one of 2 mm diameter × 30 mm length to obtain the form factor accurately and so to determine absolute resistivity values; and one of 0.33 mm diameter × 140 mm length, with greater resistance, for thermal kinetic experiments.

For the kinetic studies, the heat treatments were performed in a vertical furnace surmounting a cryostat filled with liquid helium under normal pressure. The warming-up process took place under a helium atmosphere, with a heating-up time constant of 50 s, then, during the anneals, the sample was under a 6×10^{-5} Torr pressure. After the initial temperature stabilisation, the long-time fluctuations were smaller than ±0.1 K. After annealing, the specimen was quenched by introducing cold helium gas and rapidly lowering the sample in a region where the temperature was around 77 K. Initial quench

rates were about 100 K s^{-1}. Subsequently it was placed in the 4.2 K liquid helium bath in order to measure the electrical resistivity.

For the measurements, a constant current of 0.1 A (stability of about 10^{-6}) was sent through the sample and the voltage drop between two spot-welded potential wires was measured with a seven-digit voltmeter. The measurement accuracy was 1×10^{-9} Ω cm. This relatively large uncertainty may be related to the magnetic structures obtained during the electrical resistivity measurement at 4.2 K. Since the samples are ferromagnetic, small variations of the strain state can considerably affect the magnetic domain configuration and thus the magnetoresistance contribution to the electrical resistivity values. This effect has been clearly identified during another experimental study on the same alloys (Dimitrov *et al* 1990), in which the experimental data were more reproducible by using a 0.1 T external field during the measurement in order to suppress the domain structure. No difference in the resistivity changes was detected, within experimental uncertainty, for the measurements made with or without an applied magnetic field.

Three types of heat treatments were performed on the samples for investigating their SRO kinetics:

(i) isochronal treatments for determining the sign of the resistivity variations and the temperature range of adequate atomic mobility;

(ii) isothermal treatments after a small change in annealing temperature to investigate the kinetic laws controlling the SRO relaxation and to determine the characteristic relaxation times; and

(iii) so-called 'cross-over experiments', in which the samples are first treated to obtain a given resistivity value and then brought to the temperature at which this resistivity is the equilibrium resistivity (Trieb and Veith 1978). If the SRO states are entirely defined by the resistivity value, the resistivity should then remain constant. (This will be the case when, for instance, the structure of the alloy moves from one SRO state to another one through a series of SRO equilibrium states.) Otherwise, if two or more processes with different time constants contribute to resistivity, the experimental data will first deviate from the initial value and then go back to it.

3. Results

A series of isochronal anneals (Δt = 30 min) at successively increasing temperatures was performed on the two Ni(Al) alloys after a preliminary normalisation treatment (30 min at 1273 K followed by furnace cooling, under a 10^{-6} Torr vacuum). Figure 1 shows the observed changes in residual resistivity. First, the values remain constant, then between 600 K and about 700 K resistivity increases (slightly for the 6 at.% Al), indicating that the mobility of the thermal vacancies becomes high enough to allow changes in SRO to take place. Next, the resistivity decreases (strongly for the 10 at.% Al) up to temperatures around 850 K. In this temperature range the isochronal time interval of 30 min is sufficient to achieve equilibrium values of SRO, and the quenching rate is fast enough to retain the structure at low temperatures (this is confirmed by the agreement between these values and the equilibrium resistivities, deduced from the isothermal anneals presented below). At higher annealing temperatures a tendency to saturation of the electrical resistivity is observed: the quenching rate is then too slow for retaining equilibrium SRO at 4.2 K. Therefore, from the isochronal behaviour the following conclusions can be drawn:

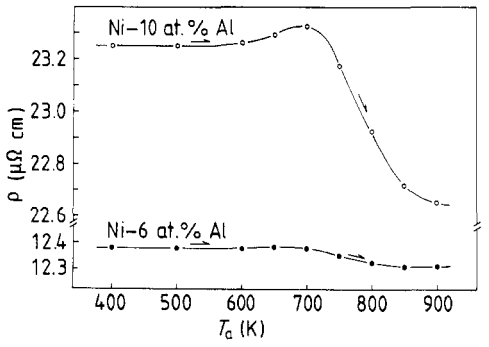

Figure 1. 4.2 K resistivity variations during isochronal anneals ($\Delta t = 30$ min) at increasing temperatures in the Ni–6 at.% Al (●) and Ni–10 at.% Al (○) alloys after normalisation treatment (30 min at 1273 K and furnace cooling).

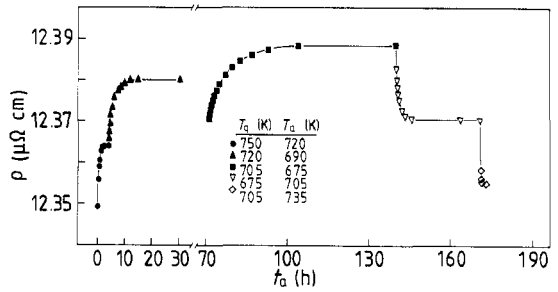

Figure 2. Residual resistivity versus annealing time for Ni–6 at.% Al alloy after small changes of the annealing temperature T_a (T_q is the quenching temperature, at which the previous anneal was performed).

(i) A decrease in SRO, promoted by the increase in annealing temperature, leads to a decrease of residual resistivity in the two alloys.

(ii) The change of electrical resistivity due to the variation in the degree of SRO increases strongly with increasing Al content (resistivity decreases by 0.5% for Ni–6 at.% Al and 3.0% for Ni–10 at.% Al between 700 and 900 K). Consequently the accuracy of resistivity variation measurements after a given annealing treatment will be clearly reduced for the smaller Al concentration.

(iii) The temperature range in which kinetics can be studied in reasonable times is centred around 700 K.

During isothermal annealing the residual resistivity evolutions plotted in figures 2 and 3 for respectively the Ni–6 at.% Al and 10 at.% Al alloys were obtained. With the small selected temperature changes, $\Delta T = \pm 30$ K for the 6 at.% Al and $\Delta T = \pm 30$ K or $+15$ K for the 10 at.% Al alloy, the resistivity variations are significant and the vacancy concentration should reach its thermal equilibrium value rapidly at the annealing temperature T_a. In every case, the resistivity, and thus the SRO, increases in down-quenching experiments ($T_q > T_a$) and decreases in up-quenching ($T_q < T_a$) experiments, starting from the pre-quench value and approaching the equilibrium value at temperature T_a.

A normalised representation, i.e. $(\rho - \rho_0)/(\rho_e - \rho_0)$ where ρ_0 is the initial and ρ_e the equilibrium resistivity, as a function of the logarithm of the annealing time t, is given in figures 4 and 5. In the Ni–6 at.% Al alloy (figure 4), where the difference $|T_q - T_a|$ was constant, the rate at which relaxation occurs, i.e. the position of the curve on the

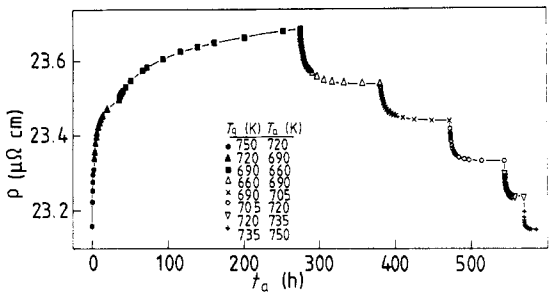

Figure 3. Same as figure 2, for the Ni–10 at.% Al alloy.

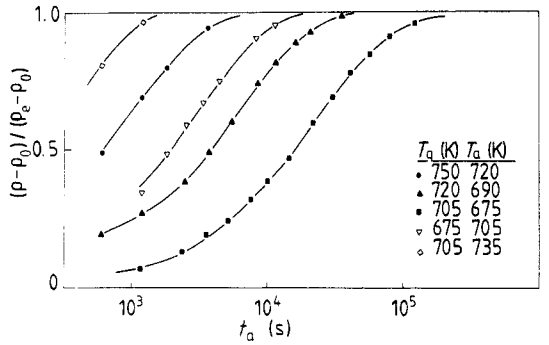

Figure 4. Normalised residual resistivity changes versus annealing time in the Ni–6 at.% Al alloy.

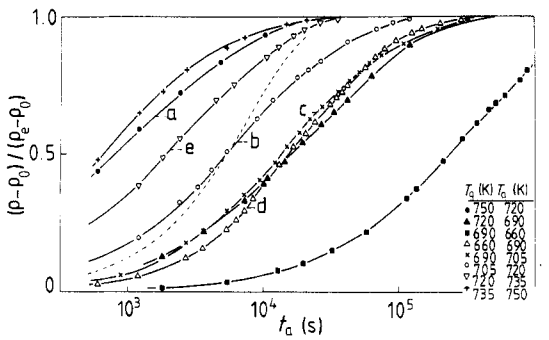

Figure 5. Same as figure 4, for the Ni–10 at.% Al alloy. The broken curve shows first-order kinetics for comparison. Curves a–e are discussed in the text.

time scale, depends only on T_a. Therefore the SRO kinetic curves are shifted progressively to longer times by a decrease in the annealing temperature. However, this is clearly not the case for the data obtained in the Ni–10 at.% Al alloy. Indeed the position of some curves (figure 5) indicates the following:

(i) At the same annealing temperature of 720 K, the evolution is faster for curve a with $\rho_e - \rho_0 = 0.161\ \mu\Omega$ cm ($T_a - T_q = -30$ K) than for curve b with $\rho_e - \rho_0 = -0.105\ \mu\Omega$ cm ($T_a - T_q = +15$ K), i.e. for the larger relaxation amplitude.

(ii) The relaxation rate is similar for curves c ($T_a = 705$ K) and d ($T_a = 690$ K), since the effect of the higher annealing temperature in curve c is approximately compensated by the smaller relaxation amplitude ($\rho_e - \rho_0 = -0.098\ \mu\Omega$ cm, instead of $-0.146\ \mu\Omega$ cm for curve d).

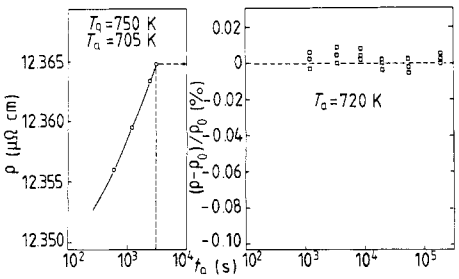

Figure 6. Cross-over experiment on Ni–6 at.% Al alloy. The initial resistivity for the 720 K anneal is the resistivity at which the 705 K was stopped.

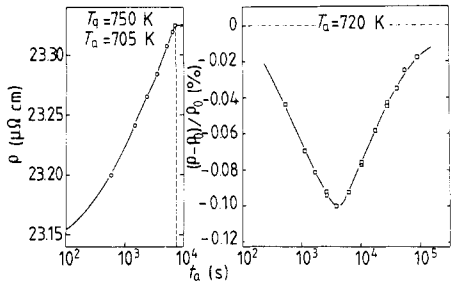

Figure 7. Same as figure 6, on the Ni–10 at.% Al alloy.

(iii) The case of curves a and e is even more striking: the time required to achieve a given fraction of the total resistivity change is shorter at 720 K for curve a with $\rho_e - \rho_0 = 0.161\ \mu\Omega$ cm ($T_a - T_q = -30$ K) at 735 K than for curve e with $\rho_e - \rho_0 = -0.0952\ \mu\Omega$ cm ($T_a - T_q = +15$ K).

So from these different observations it can be concluded that the annealing temperature T_a is not the only relevant parameter. A significant effect of the process amplitude, $\rho_e - \rho_0$, is clearly apparent: the larger the amplitude, the faster the relaxation appears (no significant effect of the sign of the resistivity change is detected, i.e. no difference between up- and down-quenching).

Cross-over experiments were also performed. The same procedure was applied to the two Al contents. A sample with the SRO equilibrium state of 750 K was annealed at 705 K until a resistivity corresponding to the equilibrium value at 720 K was reached. Then the thermal treatment was continued at the new temperature of 720 K. For the lower Al concentration, no significant effect of the temperature change was resolved. Only small dispersions around the equilibrium value at 720 K were observed, which do not indicate the existence of a cross-over effect (figure 6). On the other hand, the resistivity variations for the Ni–10 at.% Al alloy during the annealing at 720 K were much larger than experimental uncertainty (figure 7). This suggests that in the Ni–10 at.% Al alloy the relaxation behaviour is complex and involves the operation of processes with more than one relaxation time.

4. Quantitative evaluation of results

4.1. Equilibrium resistivity values

Residual resistivity values corresponding to the equilibrium state of order at each annealing temperature T_a were obtained either from the stationary resistivity achieved at long times, or by extrapolating to zero variation rate a plot of $d\rho/dt$ against $\Delta\rho$. For some annealing temperatures the stability of SRO has been checked: the equilibrium

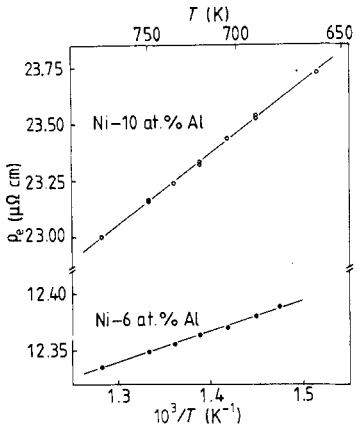

Figure 8. Equilibrium residual resistivity versus reciprocal temperature in the Ni–6 at.% Al (●) and Ni–10 at.% Al (○) alloys.

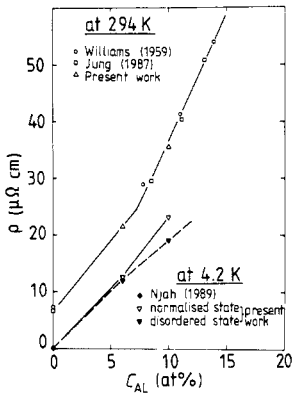

Figure 9. Resistivity at 294 K and 4.2 K versus Al concentration in Ni(Al) solid solutions.

values are independent of the previous thermal treatments. Equilibrium residual resistivity was found to vary linearly with reciprocal temperature for the two investigated alloys (figure 8) following the relations:

$$\rho_e(\mu\Omega\ \text{cm}) = (11.99 \pm 0.01) + (270 \pm 3)/T(\text{K}) \qquad \text{for Ni–6 at.\% Al} \tag{1}$$

and

$$\rho_e(\mu\Omega\ \text{cm}) = (18.93 \pm 0.06) + (3170 \pm 42)/T(\text{K}) \qquad \text{for Ni–10 at.\% Al.} \tag{2}$$

These equations provide a determination of the characteristic electrical resistivity, at 4.2 K, of the completely disordered state (corresponding to infinite temperature) of the Ni–6 at.% Al and the Ni–10 at.% Al alloys, respectively, equal to 11.99 and 18.93 $\mu\Omega$ cm. From these two values the parameter of Nordheim's relationship for single-phase disordered alloys can be calculated. So, the residual resistivity of Ni(Al) disordered alloys as a function of the atomic concentrations C_{Ni} and C_{Al} is

$$\rho_{dis}(\mu\Omega\ \text{cm}) = \rho_{Ni} + (211 \pm 1)C_{Ni}C_{Al} \tag{3}$$

with $\rho_{Ni}(\mu\Omega\ \text{cm}) = 0.008 \pm 0.001$ (Njah 1989).

The dependence of resistivity versus Al concentration is shown in figure 9. The values obtained in the present work at 294 K are in agreement with literature data (Williams 1959, Jung *et al* 1987) obtained after fast quenching from high temperature to avoid γ' precipitation. According to Jung *et al* (1987), the increasing slope, $d\rho/dC$, from about 7.5 at.% Al may indicate some initial stage of γ' precipitation. By contrast, our results show that the resistivity of the disordered Ni(Al) solid solution can be well represented by a linear relationship between ρ and $C_{Al}(1 - C_{Al})$, and that the positive deviations usually observed can be entirely explained by the effect of SRO formation.

4.2. Ordering kinetics

4.2.1. Formal kinetic laws. For a vacancy diffusion mechanism, the frequency of atomic ordering jumps, τ^{-1}, is directly proportional to the vacancy concentration, c_v, and the jump frequency, ν_v, with an efficiency factor α:

$$\tau^{-1}(s^{-1}) = \alpha c_v \nu_v. \tag{4}$$

In residual resistivity studies, the rate of isothermal variations of the degree of SRO is generally considered to be proportional to a function F of the distance to equilibrium. So, the rate equation could be written

$$-d\rho/dt = \tau^{-1} F(\rho - \rho_e) \tag{5}$$

where ρ is the instantaneous resistivity and ρ_e the equilibrium resistivity. Under stationary conditions, i.e. constant concentrations of ordering defects, several different kinetic treatments are commonly used:

(i) a pure exponential, corresponding to first-order kinetics with $F(\rho - \rho_e) = \rho - \rho_e$ characterised by a unique relaxation time τ, predicted by the statistical models (Kidin and Shtremel 1961, Cook 1969);

(ii) a more complex relaxation behaviour, assuming the existence of two simultaneous processes with different relaxation times τ_1 and τ_2, which might be explained in the model of disperse order (Shtremel and Satdarova 1969, Püschl and Aubauer 1980), and written

$$(\rho - \rho_e)/(\rho_0 - \rho_e) = A \exp(-t/\tau_1) + (1 - A) \exp(-t/\tau_2) \tag{6}$$

where A is the weight of the first relaxation process;

(iii) a first-order process with a log-normal distribution of relaxation times around a mean relaxation time $\bar{\tau}$ and with a half-width of the distribution β, from a model developed by Nowick and Berry (1972) and first applied to SRO resistivity relaxation by Balanzat and Hillairet (1981), which can be written

$$(\rho - \rho_e)/(\rho_0 - \rho_e) = \int f(\ln \tau)[1 - \exp(-t/\tau)]\, d \ln \tau \tag{7}$$

with $f(\ln \tau) = 1/(\beta\sqrt{\pi}) \exp\{-[\ln(\tau/\bar{\tau})/\beta]^2\}$.

(iv) a power law, corresponding to a process order γ, with no definite physical meaning, in which $d\rho/dt$ is proportional to $(\rho - \rho_e)^\gamma$; written

$$-(d\rho/dt)/(\rho_0 - \rho_e) = \tau^{-1} |(\rho_0 - \rho_e)/B|^{\gamma - 1} [(\rho - \rho_e)/(\rho_0 - \rho_e)]^\gamma \tag{8}$$

with a unique ordering rate τ^{-1}.

This latter relation deduced from the theory of chemical reaction rates has been proposed by Schulze and Lücke (1972) assuming that the rate of change of the parameter s that characterises the degree of SRO is described by a power law, and that resistivity is a linear function of s. Here B is a proportionality factor, with the dimension of a resistivity, between the quantity s and the SRO-induced electrical resistivity ρ_s in the form

$$\rho_s = Bs \qquad \text{with} \qquad \rho_s = \rho - \rho_{dis}. \tag{9}$$

For a binary alloy, in terms of the degree of SRO, i.e. considering the other contributions (magnetic effects, changes in electronic structure) to be negligible, the residual resistivity according to Rossiter and Wells (1971) leads to the expression

$$\rho = \rho_{dis}(1 + \sum C_i \alpha_i Y_i) \qquad \text{for } i = 1 \text{ to } \infty \tag{10}$$

where α_i are the usual Cowley parameters of the C_i atoms in the ith shell at distance R_i

and Y_i an integral function depending on the Fermi wavenumber, the radius of the coordination shell and the atomic potential used.

For a number of systems (see for instance Ni–Cu, Wagner *et al* 1981), the first term ($i = 1$) dominates, so in a reasonable approximation relation (10) can be reduced to

$$\rho = \rho_{\text{dis}}(1 + C_1 \alpha_1 Y_1). \tag{11}$$

In that case, the expression for B becomes

$$B = \mathrm{d}\rho/\mathrm{d}\alpha_1 = \rho_{\text{dis}} C_1 Y_1. \tag{12}$$

4.2.2. Applications to experimental results. The qualitative analysis of the annealing curves given in section 3 distinctly shows an amplitude dependence and the existence of a cross-over effect and so demonstrates that first-order kinetics and kinetics characterised by one relaxation time are insufficient to describe the SRO-induced resistivity changes. Indeed in the case of a process with a single relaxation time, the value of electrical resistivity after the temperature change in a cross-over experiment should stay constant (see the investigations in the AgAl system by Meisterle and Pfeiler (1983)). The negative variation (such as the one obtained for Ni–10 at.% Al, figure 7) is in most experiments explained as the consequence of the simultaneous action of two processes (see Trieb and Veith (1978) for CuAl) or of three or more processes up to a continuous relaxation spectrum (see Pfeiler *et al* (1985) for CuZn). Recently, the cross-over experiment inducing resistivity changes has been Monte Carlo simulated by Gahn and Pitsch (1989). Considering the SRO reactions in the first two neighbour shells, they observed that the cross-over effect becomes easily detectable if the relaxation times of the reactions in the different shells differ by a factor of at least 2. In Ni(Al) solid solutions, it has been shown (Chassagne 1986) that for 10.5 at.% Al the absolute magnitudes of α_1 and α_2 are comparable, whereas at low aluminium contents, α_1 is much larger than α_2. This may explain why for the Ni–6 at.% Al alloy studied in the present work the existence of a cross-over could not be significantly proved. The applicability of the above kinetic relations, which include several parameters (those in paragraphs (ii)–(iv) of section 4.2.1), is now considered.

In table 1, characteristic parameters obtained either by least-mean-squares fit of equation (6) or by comparison with tabulated theoretical curves according to equation (7) are listed. Satisfactory fits are obtained except for the larger temperature intervals ($\Delta T = \pm 30$ K) for which the ordering appears to proceed at a different rate in the initial part, below 30% of the total SRO variations, than expected from the long-time behaviour. This could be due to a non-equilibrium vacancy concentration at short annealing times. The correlation between vacancy concentrations and the ordering rates at the beginning of annealing will be further discussed after presentation of the results of the power-law kinetics.

For the Ni–10 at.% Al alloy, Arrhenius plots are given in figure 10, for τ_1 and τ_2 obtained according to equation (6), and in figure 11, for $\bar{\tau}$ corresponding to equation (7). These graphs clearly show two groups of relaxation times τ_1, τ_2 or $\bar{\tau}$, one corresponding to the smaller difference ΔT between quenching and annealing temperature and the other one to the larger ΔT. In addition, the slopes obtained from linear regressions of the data, i.e. the activation enthalpies deduced from such plots, change considerably both with the relaxation amplitude and with the method of analysis chosen. Therefore it is difficult, with these two methods, to deduce a meaningful value of the activation enthalpy.

Table 1. Kinetic parameters derived from resistivity data according to a sum of two exponentials (equation (6)) (A, τ_1 and τ_2) and a log-normal distribution of relaxation time (equation (7)) (β and $\bar{\tau}$).

C_{Al} (at.%)	T_a (K)	$T_a - T_q$ (K)	A	τ_1 (s)	τ_2 (s)	β	$\bar{\tau}$ (s)
6.0	720	−30	0.35	$(4.1 \pm 0.5) \times 10^2$	$(1.5 \pm 0.1) \times 10^3$	0.75	$(9.5 \pm 0.6) \times 10^2$
	705	+30	0.35	$(1.4 \pm 0.4) \times 10^3$	$(4.2 \pm 0.3) \times 10^3$	0.75	$(2.8 \pm 0.3) \times 10^3$
	690	−30	0.30	$(1.8 \pm 0.4) \times 10^3$	$(9.0 \pm 0.5) \times 10^3$	0.75	$(6.2 \pm 0.4) \times 10^3$
	675	−30	0.45	$(1.2 \pm 0.2) \times 10^4$	$(4.2 \pm 0.3) \times 10^4$	1.00	$(2.2 \pm 0.2) \times 10^4$
10.0	750	+15	0.65	$(5.4 \pm 0.1) \times 10^2$	$(4.5 \pm 0.1) \times 10^3$	1.75	$(1.0 \pm 0.3) \times 10^3$
	735	+15	0.50	$(1.1 \pm 0.1) \times 10^3$	$(8.5 \pm 0.4) \times 10^3$	1.75	$(3.1 \pm 0.4) \times 10^3$
	720	+15	0.55	$(3.4 \pm 0.1) \times 10^3$	$(3.5 \pm 0.1) \times 10^4$	1.75	$(7.9 \pm 0.5) \times 10^3$
		−30	0.60	$(5.7 \pm 0.2) \times 10^2$	$(5.7 \pm 0.3) \times 10^3$	1.50	$(1.6 \pm 0.4) \times 10^3$
	705	+15	0.45	$(7.5 \pm 0.1) \times 10^3$	$(5.2 \pm 0.1) \times 10^4$	1.75	$(2.0 \pm 0.2) \times 10^4$
	690	+30	0.50	$(1.0 \pm 0.1) \times 10^4$	$(5.3 \pm 0.1) \times 10^4$	1.50	$(2.2 \pm 0.3) \times 10^4$
		−30	0.45	$(0.9 \pm 0.1) \times 10^4$	$(8.9 \pm 0.3) \times 10^4$	1.75	$(2.5 \pm 0.2) \times 10^4$
	660	−30	0.40	$(0.4 \pm 0.2) \times 10^4$	$(7.3 \pm 0.5) \times 10^5$	1.75	$(3.8 \pm 0.3) \times 10^5$

Accuracy: $\Delta A = \pm 0.05$ and $\Delta\beta = \pm 0.15$.

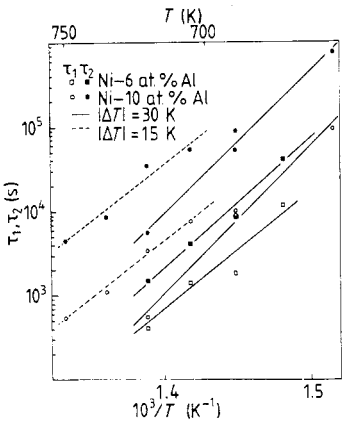

Figure 10. Arrhenius diagram of the relaxation times τ_1 and τ_2 according to table 1.

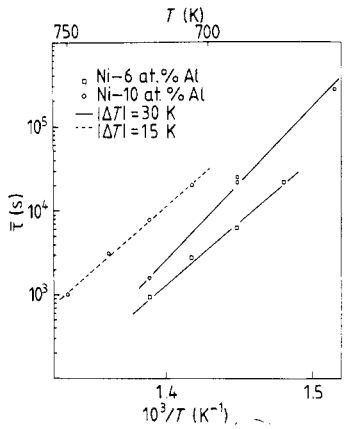

Figure 11. Arrhenius diagram of the mean relaxation time $\bar{\tau}$ according to table 1.

We consider now the last presented model in the previous section. The experimental points are plotted in figure 12 according to the power-law equation (8) for the Ni–6 at.%Al alloy and in figure 13 for Ni–10 at.%Al. These diagrams have to be read from right to left. In the representation of the logarithm of the relaxation rate versus logarithm of the deviation from equilibrium, straight lines with intercepts $\ln(\tau^{*-1})$, with

$$\tau^{*-1} = |(\rho_0 - \rho_e)/B|^{\gamma-1}\tau^{-1} \tag{13}$$

and slope γ are expected for a constant vacancy concentration. Actually initial deviations from the linear plots occur for all 30 K quenching intervals $|T_q - T_a|$ and can be attributed to changes of vacancy concentration at short annealing times. Since the ordering or

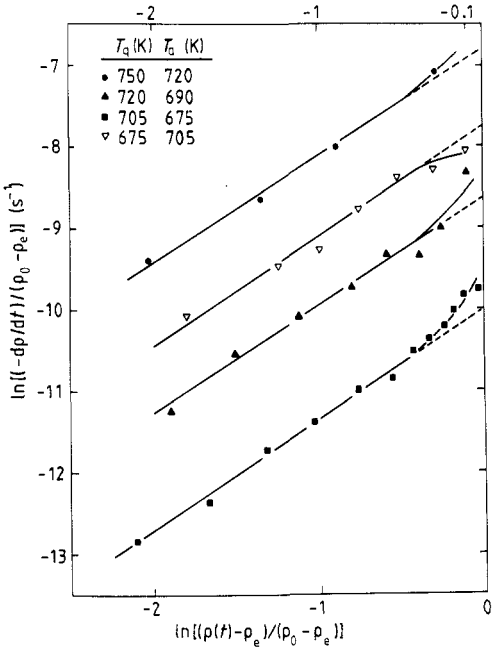

Figure 12. Normalised rate of resistivity change $(-d\rho/dt)/(\rho_0 - \rho_e)$ versus normalised distance to equilibrium $(\rho - \rho_e)/(\rho_0 - \rho_e)$ for the Ni–6 at.% Al alloy.

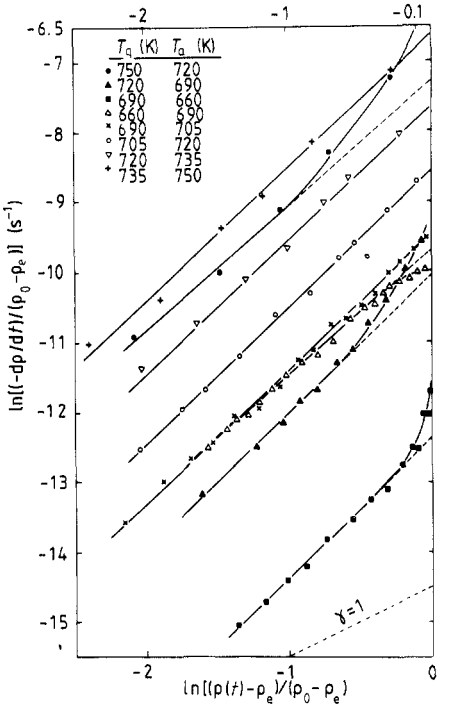

Figure 13. Same as figure 12, for the Ni–10 at.% Al alloy.

disordering rates should be proportional to the product of vacancy concentration and jump frequency, equation (4), the initial positive deviations in the down-quenching experiments and the negative ones in the up-quenching experiments respectively reflect the excess and the deficiency of vacancies with respect to the equilibrium vacancy concentration at the annealing temperature. Such deviations were observed and similarly explained in a NiCr alloy by Heidsiek *et al* (1982). Consequently, the values of τ^{*-1} were determined by extrapolating to $(\rho - \rho_0)/(\rho_0 - \rho_e) = 1$ the straight lines obtained by linear fits of the data corresponding to sufficiently long annealing times.

In figure 13, the amplitude effects described in section 3 also exist and lead to comparable remarks about the position of the curves in terms of annealing temperature and of magnitude of $T_q - T_a$.

All the parameters derived from the resistivity data by linear least-squares fits of the kinetic power law for the two investigated alloys are given in table 2. With the values of the resistivity amplitude $\rho_0 - \rho_e$, the exponent γ and the initial intercepts, the characteristic relaxation times τ for each annealing temperature have been calculated according to equation (13). For the 10 at.%Al alloy, the B constant was determined by using the α_1 parameter obtained by Chassagne (1986) at 823 K. Since no such data were available for the 6 at.%Al alloy, the required α_1 value was evaluated by assuming that α_1 was proportional to the Al concentration. The resulting τ values have been plotted in an Arrhenius graph (figure 14). By contrast with the relaxation times obtained from

Table 2. Kinetic parameters derived from resistivity data according to a power law (equation (8)).

C_{Al} (at.%)	T_a (K)	$\rho_0 - \rho_e$ ($\mu\Omega$ cm)	γ	$\ln[\tau^{*-1}(s^{-1})]$	τ (s)
6.0	720	−0.0151	1.30 ± 0.10	−6.80 ± 0.10	(1.5 ± 0.1) × 10^2
	705	+0.0182	1.35 ± 0.10	−7.80 ± 0.10	(3.2 ± 0.3) × 10^2
	690	−0.0177	1.30 ± 0.10	−8.60 ± 0.10	(9.5 ± 0.2) × 10^2
	675	−0.0188	1.40 ± 0.05	−9.95 ± 0.05	(2.1 ± 0.1) × 10^3
10.0	750	+0.0880	1.85 ± 0.05	−6.65 ± 0.10	(4.1 ± 0.1) × 10^0
	735	+0.0952	1.90 ± 0.05	−7.65 ± 0.05	(8.8 ± 0.1) × 10^0
	720	+0.1052	1.95 ± 0.05	−8.55 ± 0.05	(1.8 ± 0.2) × 10^1
		−0.1613	1.75 ± 0.10	−7.30 ± 0.15	(2.3 ± 0.6) × 10^1
	705	+0.0980	1.90 ± 0.05	−9.50 ± 0.05	(5.7 ± 0.1) × 10^1
	690	+0.1461	1.80 ± 0.05	−9.70 ± 0.05	(1.8 ± 0.2) × 10^2
		−0.2046	1.95 ± 0.10	−10.00 ± 0.10	(1.4 ± 0.3) × 10^2
	660	−0.2314	2.00 ± 0.05	−12.35 ± 0.05	(1.3 ± 0.2) × 10^3

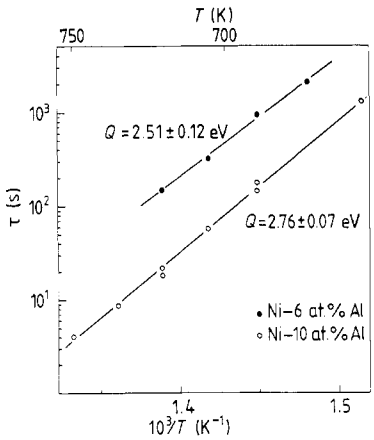

Figure 14. Arrhenius diagram of the relaxation time τ according to table 2.

the two previously considered models, the present data give consistent results for all annealing temperatures and especially for the Ni–10 at.%Al, irrespective of the initial relaxation amplitude. So for each alloy a unique straight line is obtained according to $\tau = \tau_0 \exp(Q/kT)$. Their slopes yield the corresponding activation enthalpies. The characteristic parameters of the Arrhenius laws of amplitude-corrected time constants were found as:

$Q(\text{eV}) = 2.51 \pm 0.12$ and $5 \times 10^{-17} < \tau_0(\text{s}) < 3 \times 10^{-15}$ for Ni–6 at.%Al

$Q(\text{eV}) = 2.76 \pm 0.07$ and $3 \times 10^{-19} < \tau_0(\text{s}) < 3 \times 10^{-18}$ for Ni–10 at.%Al.

The results, compared to literature diffusion data for Ni(Al) solutions, are listed in table 3. The present activation enthalpy values lie in the same range as published ones, although they were obtained in a much lower temperature interval. Taking into account measurement accuracy, the variation of activation enthalpy with aluminium concentration in the present alloys can be considered as significant and the activation

Table 3. Diffusion data in nickel-rich solutions.

Material	Diffusion type	Activation enthalpy (eV/atom)	Temperature range (K)	Reference
Ni	Self-diffusion	2.88	813 to 1193	Maier *et al* (1976)
Al in Ni	Impurity diffusion	2.70 ± 0.14	914 to 1212	Gust *et al* (1981)
		2.58	1073 to 1243	Allison and Samelson (1959)
Ni(Al)	Interdiffusion	2.42 ± 0.12	1223 to 1423	Shankar and Seigle (1978)
		2.82 ± 0.09	1223 to 1573	Janssen (1973)
Ni–6 at.% Al	Self-diffusion	2.51 ± 0.12	675 to 720	Present work
Ni–10 at.% Al		2.76 ± 0.07	660 to 750	

enthalpy value seems to go through a minimum between pure nickel and the Ni–10 at.%Al alloy.

An interesting consequence of the present results is the possibility of predicting the effective time constant for ordering τ^*, for a given set of experimental conditions. Indeed, from this value, the adequate annealing time to attain the equilibrium state can be determined. For instance, this parameter is useful in x-ray diffuse scattering experiments in which the SRO state is generally investigated as a function of the annealing temperature. So, if the initial state corresponds to the equilibrium state at the quenching temperature T_q, a relation between τ^*, T_q and T_a is deduced from the previous equation (13) and from the temperature equilibrium resistivity dependence (equations (1) and (2), section 4.1):

$$\tau^* = 9 \times 10^{-17}(T_a T_q/|T_a - T_q|)^{0.35} \exp(2.51/kT_a) \qquad \text{for Ni–6 at.\% Al}$$

$$\tau^* = 2 \times 10^{-20}(T_a T_q/|T_a - T_q|)^{0.90} \exp(2.76/kT_a) \qquad \text{for Ni–10 at.\% Al}$$

where 0.35 and 0.90 are the average values of $(\gamma - 1)$ for each alloy.

Some remarks can be made about these values of the reaction orders. In the two alloys, when the effect of the variations of vacancy concentration is correctly excluded during the isothermal experiments, a single value of γ for each Al content characterises the SRO formation controlled by thermal diffusion. So the exponent γ can be considered as a kind of material constant. Nevertheless the problem is to understand why just these two values are obtained and what their physical meaning is. A comparison between the results from the different models considered in the present paper shows a correlation between the variation of γ and of β. The small value of γ for Ni–6 at.% Al and the large value of γ for Ni–10 at.% Al are respectively associated with a small and a large value of β, in agreement with the empirical correspondence between these two parameters presented by Balanzat and Halbwachs (1983). Furthermore, we have seen above that aluminium concentrations also had an influence on the amplitude of the cross-over effect. These two observations might have the same origin, namely the relative importance of the contributions of the first two Warren–Cowley SRO parameters to the electrical resistivity variations. In the case where one of these contributions is strongly dominant, it is expected that the relaxation will proceed in a narrow time interval (low γ or β values) and little cross-over will occur. By contrast if α_1 and α_2 are comparable weights, with different time constants, the relaxation will be spread out on the time scale (large γ or β values) and a cross-over effect will be obtained.

5. Conclusions

Significant variations of SRO can be obtained and accurately characterised by residual electrical resistivity measurements in Ni–6 at.% Al and 10 at.% Al alloys. The formation of SRO in these solid solutions increases electrical resistivity and this effect is much more important for the higher Al concentration. The equilibrium residual resistivity, obtained after long isothermal anneals, is a linear function of reciprocal temperature.

The study of SRO kinetics shows an effective influence of the relaxation amplitude. This excludes a quantitative analysis by first-order kinetics, including the case of a distribution of relaxation times. The model of the sum of two exponentials could in principle represent such an effect. However, in the present case, it does not lead to a unique relationship between the temperature and the relaxation times. Only the power-law approach gives consistent results for the temperature dependence of the relaxation time, but it cannot represent the results of cross-over experiments (observed in the Ni–10 at.% Al alloy). The values of the shape parameters of the SRO kinetic laws (ii) and (i) and the existence of a cross-over phenomenon have been correlated with the importance of the relative contributions of the first two atomic shells, as a function of the Al concentration. The obtained self-diffusion enthalpies appear to increase between 6 at.% Al to 10 at.% Al and are in the same range as published diffusion data.

Acknowledgment

The authors would like to express their gratitude to the Société Nationale d'Etude et de Construction de Moteurs d'Aviation for financial support of this work.

References

Afyouri M, Cadeville M C, Pierron-Bohnes V and Vennegues P 1989 *Defects and Diff. Forum* **66–69** 1449
Allison H W and Samelson H 1959 *J. Appl. Phys.* **30** 1419
Balanzat E and Halbwachs M 1983 *Phys. Status Solidi* a **76** 667
Balanzat E and Hillairet J 1981 *J. Phys. F: Met. Phys.* **11** 1977
Chassagne F 1986 *Thesis* University of Paris VI
Cook H E 1969 *J. Phys. Chem. Solids* **30** 2427
Cowley J M 1950 *J. Appl. Phys.* **21** 24
Dimitrov C, Zhang X, Sitaud B, Dimitrov O, Dedek U and Dworschak F 1989 *European Conf. on Advanced Materials and Processes, Euromat 89, (Aachen, 1989)* Communication IV 5.
Gahn U and Pitsch W 1989 *Acta Metall.* **37** 391
Gust W, Hintz M B, Lodding A, Odelius H and Predel B 1981 *Phys. Status Solidi* a **64** 187
Guy A G 1962 *Trans. ASM* **55** 737
Hansen M and Anderko K 1958 *Constitution of Binary Alloys* 2nd edn (New York: McGraw-Hill) p 118
Heidsiek H, Lücke K and Scheffel R 1982 *J. Phys. Chem. Solids* **43** 825
Janssen M M P 1973 *Metall. Trans.* **4** 1623
Jung P, Ansari M I, Klein H and Meertens D 1987 *J. Nucl. Mater.* **148** 148
Katsnel'son A A, Silonov A M and Silonov V M 1972 *Fiz. Metal. Metalloved.* **33** 1267
—— 1977 *Fiz. Metal. Metalloved.* **44** 650
Kidin I I and Shtremel M A 1961 *Fiz. Metal. Metalloved.* **11** 64
Klaiber F, Schönfeld B and Kostorz G 1987 *Acta Crystallogr.* A **43** 525
Maier K, Mehrer H, Lessman E and Schüle W 1976 *Phys. Status Solidi* b **78** 689
Meisterle P and Pfeiler W 1983 *Acta Metall.* **31** 1543
Njah N 1989 *Thesis* University of Paris VI

Nowick A S and Berry B S 1972 *Anelastic Relaxation in Crystalline Solids* (New York: Academic Press)
Pfeiler W, Reihsner R and Trattner D 1985 *Scr. Metall.* **19** 199
Püschl W and Aubauer H P 1980 *Phys. Status Solidi* b **102** 447
Rossiter P L and Wells P 1971 *J. Phys. C: Solid State Phys.* **4** 354
Sanchez J M, Barefoot J R, Jarrett R N and Tien J K 1984 *Acta Metall.* **32** 1519
Schulze A and Lücke K 1972 *Acta Metall.* **20** 529
Shankar S and Seigle L L 1978 *Metall. Trans.* **9A** 146
Shtremel M A and Satdarova F F 1969 *Fiz. Metal. Metalloved.* **27** 396
Starke E A, Gerold V and Guy A G 1965 *Acta Metall.* **13** 957
Trieb L and Veith G 1978 *Acta Metall.* **26** 185
Wagner W, Poerschke R and Wollenberger H 1981 *Phil. Mag.* B **43** 345
Williams R O 1959 *Trans. AIME* **215** 1026